EMBO reports

scientific report

Regulation of PI(3)K/Akt signalling and cellular transformation by inositol polyphosphate 4-phosphatase-1

Ivan Ivetac[1], Rajendra Gurung[1], Sandra Hakim[1], Kristy A. Horan[1], David A. Sheffield[1], Lauren C. Binge[1], Philip W. Majerus[2], Tony Tiganis[1] & Christina A. Mitchell[1+]

[1]Department of Biochemistry, Monash University, Clayton, Victoria, Australia, and [2]Department of Hematology, Washington University, St Louis, Missouri, USA

Akt is a crucial phosphoinositide 3-kinase (PI(3)K) effector that regulates cell proliferation and survival. PI(3)K-generated signals, PtdIns(3,4,5)P_3 and PtdIns(3,4)P_2, direct Akt plasma membrane engagement. Pathological Akt plasma membrane association promotes oncogenesis. PtdIns(3,4)P_2 is degraded by inositol polyphosphate 4-phosphatase-1 (4-ptase-1) forming PtdIns(3)P; however, the role of 4-ptase-1 in regulating the activation and function of Akt is unclear. In mouse embryonic fibroblasts lacking 4-ptase-1 ($^{-/-}$MEFs), the Akt-pleckstrin homology (PH) domain was constitutively membrane-associated both in serum-starved and agonist-stimulated cells, in contrast to $^{+/+}$MEFs, in which it was detected only at the plasma membrane following serum stimulation. Epidermal growth factor (EGF) stimulation resulted in increased Ser^{473} and Thr^{308}-Akt phosphorylation and activation of Akt-dependent signalling in $^{-/-}$MEFs, relative to $^{+/+}$MEFs. Significantly, loss of 4-ptase-1 resulted in increased cell proliferation and decreased apoptosis. SV40-transformed $^{-/-}$MEFs showed increased anchorage-independent cell growth and formed tumours in nude mice. This study provides the first evidence, to our knowledge, that 4-ptase-1 controls the activation of Akt and thereby cell proliferation, survival and tumorigenesis.

Keywords: PI(3)-kinase; Akt; 4-phosphatase; oncogenesis

EMBO reports (2009) **10**, 487–493. doi:10.1038/embor.2009.28

INTRODUCTION

The serine-threonine kinase, Akt, is a crucial phosphoinositide 3-kinase (PI(3)K) effector (Manning & Cantley, 2007), and the association of Akt at the plasma membrane is crucial for its activation. Transforming mutations in the Akt1-pleckstrin homology (PH) domain lead to its pathological plasma membrane association and to the malignant transformation of cells (Carpten *et al*, 2007). In response to growth factor stimulation, PI(3)Ks generate PtdIns(3,4,5)P_3 and PtdIns(3,4)P_2 at the plasma membrane, which bind to the PH domain of Akt resulting in 'catalytic T-loop' phosphorylation on Thr^{308} by 3-phosphoinositide-dependent kinase 1 (PDK1). The hydrophobic motif of Akt is phosphorylated on Ser^{473} by mammalian target of rapamycin complex 2 (mTORC2). Active Akt phosphorylates many cytosolic targets that promote cell proliferation and inhibit apoptosis (Sarbassov *et al*, 2005; Engelman *et al*, 2006).

PtdIns(3,4,5)P_3 is a short-lived signal that is degraded by two main pathways. The tumour suppressor, phosphatase and tensin homologue deleted on chromosome 10 (PTEN), hydrolyses PtdIns(3,4,5)P_3 to form PtdIns(4,5)P_2 (Tamguney & Stokoe, 2007); however, PtdIns(3,4,5)P_3 is also hydrolysed by inositol polyphosphate 5-phosphatases to form PtdIns(3,4)P_2, which is, in turn, degraded by inositol polyphosphate 4-phosphatases (4-ptases) to generate PtdIns(3)P (Stephens *et al*, 1993; Astle *et al*, 2006). Two 4-ptases, type-1 and 2, have been identified (Norris *et al*, 1995, 1997). A spontaneously occurring murine mutation designated *Weeble* has been genetically linked to a point mutation in the *4-ptase-1* gene that causes a frame shift, resulting in the absence of 4-ptase-1 messenger RNA and protein (Nystuen *et al*, 2001; Ivetac *et al*, 2005). *Weeble* mice show cerebellar defects and die shortly after birth. 4-Ptase-1 specifically regulates the cellular levels of PtdIns(3,4)P_2. *In vitro* recombinant 4-ptase-1 hydrolyses PtdIns(3,4)P_2 to form PtdIns(3)P (Norris *et al*, 1995). 4-Ptase-1 overexpression in cells decreases total cellular PtdIns(3,4)P_2 but not PtdIns(3,4,5)P_3 signals (Kisseleva *et al*, 2002). 4-Ptase-1-deficient *Weeble* cells show a 2.5-fold serum-stimulated rise in PtdIns(3,4)P_2 relative to wild-type controls, but no increase in PtdIns(3,4,5)P_3 signals (Shin *et al*, 2005).

Several studies have suggested that PtdIns(3,4)P_2 might also support the activation of Akt. Increases in the activity of Akt spatio-temporally correlate with PtdIns(3,4)P_2 fluxes, and the Akt-PH domain binds to both PtdIns(3,4)P_2 and PtdIns(3,4,5)P_3

[1]Department of Biochemistry, Monash University, Wellington Road, Clayton, Victoria 3800, Australia
[2]Department of Hematology, Washington University, 660 South Euclid Avenue, St Louis, Missouri 63110, USA
[+]Corresponding author. Tel: +61 3 99053790; Fax: +61 3 99053726;
E-mail: christina.mitchell@med.monash.edu.au

Received 15 August 2008; revised 5 February 2009; accepted 5 February 2009; published online 27 March 2009

(Andjelkovic *et al*, 1997; Franke *et al*, 1997). However, the specific and/or distinct *in vivo* function of 4-ptase-1 in regulating Akt activation, signalling, and cellular responses remains unclear. Here, we report that the loss of 4-ptase-1 leads to constitutive association of the Akt-PH domain with the plasma membrane, increased activation and signalling of Akt, and increased cellular proliferation and survival, enhancing tumour formation. These studies identify that 4-ptase-1 negatively regulates PI(3)K/Akt-dependent mitogenic signalling.

RESULTS

4-Ptase-1-deficient cells show increased Akt signalling

We used *Weeble* mouse embryonic fibroblasts ($^{-/-}$MEFs) to examine 4-ptase-1 regulation of PI(3)K/Akt signalling. Immunoblot analysis revealed the absence of 4-ptase-1 in $^{-/-}$MEFs (Fig 1A) with no compensatory increase in PTEN (data not shown). Constitutive Akt plasma membrane association leads to carcinogenesis (Carpten *et al*, 2007). We investigated whether 4-ptase-1 regulates Akt plasma membrane recruitment. Primary MEFs were transfected with green fluorescent protein-Akt-PH (GFP-Akt-PH; Fig 1B) and, in some experiments, also co-transfected with mCherry (a cytosolic fluorescent protein; Fig 1C–E). Live cell imaging revealed no membrane engagement of GFP-Akt-PH in serum-starved $^{+/+}$MEFs, but patchy membrane localization following serum stimulation (Fig 1B,C). In $^{-/-}$MEFs, GFP-Akt-PH was plasma membrane associated at focal patches even in serum-starved cells with enhanced membrane association following stimulation (Fig 1B,C). Focal regions were identified that accumulated GFP-Akt-PH at the plasma membrane by time-lapse ratiometric fluorescence microscopy (Fig 1D,E). At each time point, plasma membrane GFP-Akt-PH fluorescence was expressed as a ratio of mCherry (R_{PM}) in the same area (Fig 1Diii,vi divided images) and, to standardize for fluorescence intensity, normalized relative to a GFP-Akt-PH/mCherry ratio of a defined cytosolic area (R_{CYT}), generating R_{PM}/R_{CYT} (Fig 1E; method adapted from Henry *et al*, 2004). In serum-starved $^{+/+}$MEFs, GFP-Akt-PH was cytosolic but following serum stimulation localized to focal areas at the plasma membrane (Fig 1C,Di–iii) that were not enriched in mCherry (Fig 1Dii). In $^{-/-}$MEFs, GFP-Akt-PH, but not mCherry, showed membrane engagement even in serum-starved cells (Fig 1C,Div–vi). At peak levels post-agonist stimulation (12 min), GFP-Akt-PH membrane association was similar in $^{-/-}$MEFs and $^{+/+}$MEFs; however, at all other times, membrane association was higher in $^{-/-}$MEFs (Fig 1D,E). In agonist-stimulated $^{+/+}$MEFs and serum-starved or stimulated $^{-/-}$MEFs, GFP-Akt-PH membrane engagement was PI(3)K dependent, as LY294002 treatment led to loss of membrane association (data not shown). Interestingly, the plasma membrane recruitment of PtdIns(3,4,5)P_3-specific PH domains (Btk and ARNO) for both serum-starved and stimulated conditions was similar in $^{-/-}$MEFs and $^{+/+}$MEFs (data not shown). This is consistent with the evidence that 4-ptase-1 degrades PtdIns(3,4)P_2, but not PtdIns(3,4,5)P_3 (Kisseleva *et al*, 2002; Shin *et al*, 2005). Therefore, loss of 4-ptase-1 is associated with constitutive Akt-PH domain plasma membrane association, even under adverse conditions such as serum starvation. Plasma membrane engagement of the PtdIns(3,4)P_2-specific tandem PH domain-containing protein (TAPP1)-PH domain was also evaluated. Constitutive GFP-tandem PH domain-containing protein (TAPP1)-PH association with the plasma membrane was apparent in serum-starved $^{-/-}$MEFs, but not $^{+/+}$MEFs; however, the fluorescence intensity at the plasma membrane was insufficient for ratiometric analysis (data not shown).

Constitutive Akt plasma membrane association leads to enhanced activation of Akt by phosphorylation (Andjelkovic *et al*, 1997; Carpten *et al*, 2007). Phosphorylation of Akt at Ser^{473} and Thr^{308} was increased following serum starvation in primary $^{-/-}$MEFs relative to $^{+/+}$MEFs, albeit not at statistically significant levels. Following EGF stimulation, significant 1.75- and 1.6-fold increases in pSer^{473}-Akt and Thr^{308}, respectively, were detected at 5 min, persisting for up to 180 min in $^{-/-}$MEFs relative to $^{+/+}$MEFs (Fig 2A,B). Akt downstream signalling was assessed using a pAkt substrate antibody, which detects Akt-Ser/Thr phosphorylated proteins having an 'RxRxxpS*/pT*' motif. In response to EGF, $^{-/-}$MEFs showed increased immunoreactive proteins relative to $^{+/+}$MEFs (Fig 2C). Active Akt phosphorylates many targets including the FoxO transcription factors, which regulate cell-cycle arrest, apoptosis, senescence and cellular stress responses (Manning & Cantley, 2007). In the absence of stimulation, primary $^{-/-}$MEFs showed increased pThr^{32}-FoxO3a levels (Fig 2D) relative to $^{+/+}$MEFs, which increased further following EGF stimulation. Loss of function of 4-ptase-1 therefore leads to increased and sustained growth factor-stimulated levels of pSer^{473}/Thr^{308}-Akt and Akt phospho-substrates; by contrast, activation of ERK1/2 (p44/p42) and p38 MAPK was unaltered by the deficiency of 4-ptase-1 (data not shown).

We verified that the enhanced Akt plasma membrane association and phosphorylation observed in $^{-/-}$MEFs was a consequence of the deficiency of 4-ptase-1 by reconstituting $^{-/-}$MEFs with 4-ptase-1 using retroviral transduction (Fig 3A–E). Immunoblot analysis of the level of 4-ptase-1 protein expressed in reconstituted MEFs revealed a fivefold increase relative to endogenous 4-ptase-1 in $^{+/+}$MEFs (data not shown). Akt plasma membrane recruitment was examined in fixed and digitonin-permeabilized cells using purified glutathione *S*-transferase-Akt-PH (GST-Akt-PH). In mock-reconstituted $^{-/-}$MEFs, GST-Akt-PH was localized to the plasma membrane in both serum-starved and stimulated cells (Fig 3B,D). By contrast, in 4-ptase-1-reconstituted $^{-/-}$MEFs, GST-Akt-PH was cytosolic in unstimulated cells and showed less plasma membrane association following stimulation (Fig 3A,D). Significantly, 4-ptase-1-reconstituted $^{-/-}$MEFs showed decreased EGF-stimulated pSer^{473} and Thr^{308}-Akt relative to mock-reconstituted $^{-/-}$MEFs (Fig 3E).

Deficiency of 4-ptase-1 increases cellular proliferation

Amplification of PI(3)K/Akt signalling promotes cell proliferation and anti-apoptotic signalling (Engelman *et al*, 2006). However, the function of 4-ptase-1 in regulating the mitogenic responses of PI(3)K/Akt remains unclear. To avoid possible mutations/changes introduced by cell immortalization, we performed cell proliferation and apoptosis assays on primary MEFs. Primary $^{-/-}$MEFs showed an approximate twofold reduction in the time required for cell doubling relative to $^{+/+}$MEFs or $^{+/-}$MEFs when grown in 10% fetal calf serum (FCS; Fig 4A) or when cultured in the absence of serum (Fig 4B), although all cells became non-viable by day 5 in the absence of serum. Next, we investigated the impact of 4-ptase-1 deficiency on cell survival. Serum withdrawal initiates the apoptotic programme in primary cell cultures. At 72 h post-serum withdrawal, $^{-/-}$MEFs showed lower levels of apoptosis relative to $^{+/-}$MEFs and

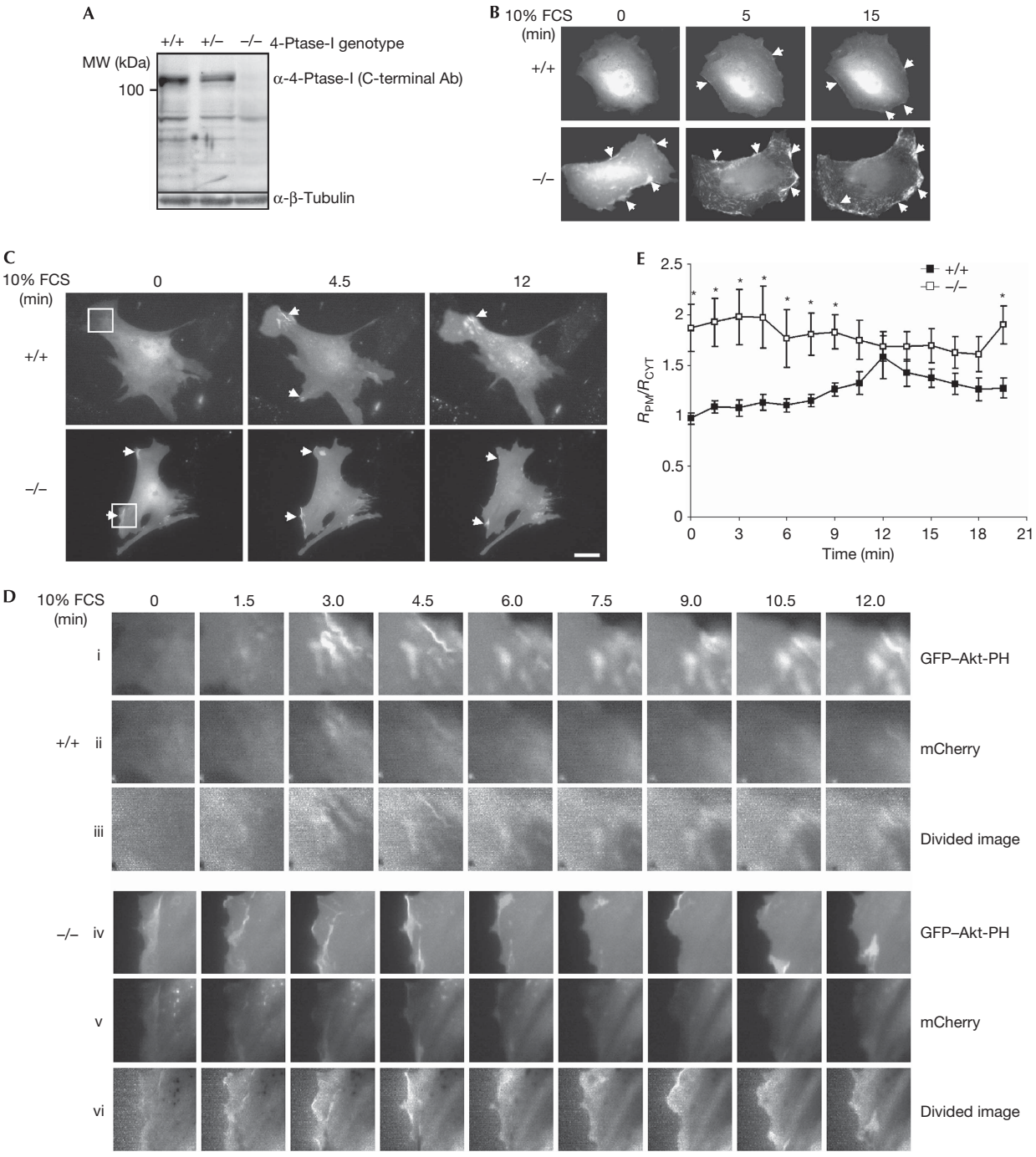

Fig 1 | Constitutive GFP-Akt-PH plasma membrane engagement in $^{-/-}$MEFs. (**A**) MEFs were immunoblotted with 4-ptase-1 or β-tubulin antibodies. (**B**) Live $^{+/+}$MEFs and $^{-/-}$MEFs were transfected with GFP-Akt-PH and (**C**) co-transfected with mCherry, serum starved followed by serum stimulation; time-lapse fluorescence microscopy was performed at 1.5-min intervals (see Methods). Arrows indicate plasma membrane localization. Scale bar, 20 μm. (**D**) Higher magnification of boxed regions in (**C**) showing (i, iv) GFP-Akt-PH, (ii, v) mCherry or (iii, vi) divided image of GFP-Akt-PH/mCherry. (**E**) R_{PM}/R_{CYT} was determined (see Methods). Data represent mean ± s.e.m. of four experiments for five $^{+/+}$MEFs and $^{-/-}$MEFs (*$P<0.05$). Ab, antibody; FCS, fetal calf serum; GFP, green fluorescent protein; MEF, mouse embryonic fibroblast; MW, molecular weight; PH, pleckstrin homology.

$^{+/+}$MEFs, as assessed by TdT-mediated dUTP nick end labelling (TUNEL) assay (Fig 4C) and activation of caspase-3 (data not shown). Similarly, on treatment with staurosporine, cycloheximide or agonistic Fas antibodies, $^{-/-}$MEFs showed reduced apoptosis relative to $^{+/+}$MEFs (Fig 4D). Growth of tumour cells is typically characterized by anchorage independence. Primary fibroblasts were immortalized by the SV40 large T antigen. Following transformation, both $^{+/+}$MEFs and $^{-/-}$MEFs showed the capacity to grow

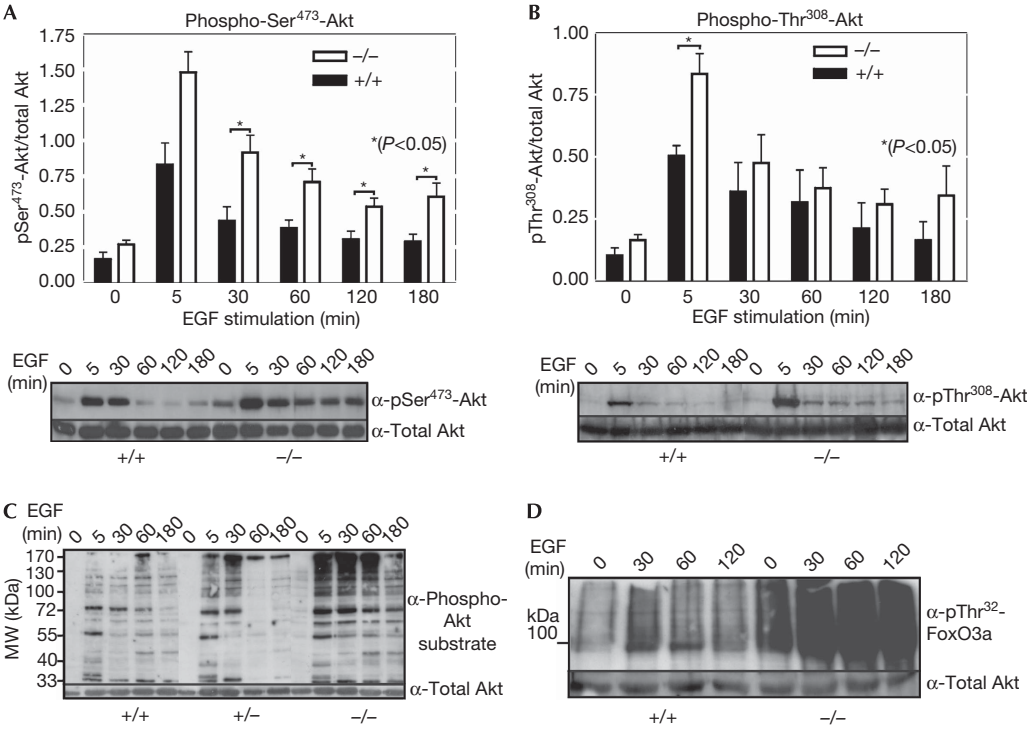

Fig 2 | Increased and sustained Akt phosphorylation in $^{-/-}$MEFs. Primary MEFs were serum-starved and stimulated with 100 ng/ml EGF and immunoblotted with (**A**) pSer^{473}-Akt ($n=6$), (**B**) pThr^{308}-Akt ($n=4$), (**C**) pAkt substrate specific and (**D**) pThr^{32}-FKHRL1 (FoxO3a) (representative of three experiments), or Akt antibodies. (**A**,**B**) Blots were analysed by densitometry and normalized to Akt protein (*$P<0.05$). All immunoblots of $^{+/+}$MEFs and $^{-/-}$MEFs were performed simultaneously under the same transfer and immunoblotting conditions. EGF, epidermal growth factor; MEF, mouse embryonic fibroblast; MW, molecular weight.

independently of anchorage; however, $^{-/-}$MEFs gave rise to significantly greater numbers of colonies in soft agar compared with $^{+/+}$MEFs (Fig 4E,F). We also evaluated the ability of SV40-transformed $^{-/-}$MEFs in comparison with $^{+/+}$MEFs to form tumours when injected subcutaneously into the flanks of nude mice (Fig 4G). By 13 weeks post-injection, four out of five mice injected with transformed $^{-/-}$MEFs developed tumours in their flanks (volume: $678 \pm 148\ mm^3$). By contrast, no tumours were detected in any of the five mice injected with transformed $^{+/+}$MEFs, indicating that 4-ptase-1 deficiency promotes tumorigenesis.

DISCUSSION

Akt phosphorylation and activation of downstream signalling is directed by its plasma membrane association (Andjelkovic *et al*, 1997; Manning & Cantley, 2007). Transforming somatic mutations in the Akt1-PH domain have been identified in breast, colorectal and ovarian cancers, which result in its pathological association with the plasma membrane, enhanced Akt phosphorylation, increased cell survival, proliferation and oncogenesis (Carpten *et al*, 2007). As shown here, 4-ptase-1 loss of function results in similar effects, including constitutive association of the Akt-PH domain with the plasma membrane, increased phosphorylation of Akt and its substrates, enhanced cell proliferation, survival and tumour formation. Constitutive Akt-PH domain engagement in $^{-/-}$MEFs might 'prime' Akt for phosphorylation following cell stimulation.

The function of 4-ptase-1 in regulating cell proliferation and/or apoptosis has been investigated only by using overexpression studies, unlike the loss-of-function approach reported here. The overexpression of 4-ptase-1 suppressed megakaryocyte and NIH3T3 cell proliferation, but had no effect on apoptosis (Vyas *et al*, 2000). Kisseleva *et al* (2002) overexpressed 4-ptase-1 in human embryonic kidney 293 cells decreasing Akt phosphorylation in quiescent cells but, paradoxically, increasing growth factor-stimulated Akt activation and resistance to Fas-induced apoptosis. In apparent disagreement, we have shown that the deficiency of 4-ptase-1 enhances EGF-stimulated pSer^{473}-Akt and pThr^{308}-Akt associated with resistance to apoptosis. In addition, the reconstitution of 4-ptase-1 in $^{-/-}$MEFs reduced EGF-stimulated pSer^{473}-Akt and pThr^{308}-Akt. A possible explanation for the apparent discrepancy between our study and that of Kisseleva *et al* is that inducible 4-ptase-1 overexpression in 293 cells decreased PtdIns(3,4)P_2 but, paradoxically, increased PtdIns(3,4,5)P_3 signals by an uncharacterized negative feedback loop. Therefore, under these experimental conditions, PtdIns(3,4,5)P_3 signals might enhance Akt phosphorylation and cell survival, independent of PtdIns(3,4)P_2 (Kisseleva *et al*, 2002). In addition, the effects of 4-ptase-1 might be cell-type specific, or relate to the level and/or duration of its overexpression.

Purified recombinant wild type, but not catalytically inactive 4-ptase-1, hydrolyses PtdIns(3,4)P_2 to form PtdIns(3)P (Norris *et al*, 1995; Ivetac *et al*, 2005). As reported here, *Weeble* MEFs, which lack 4-ptase-1, showed enhanced GFP-PH-TAPP1 plasma membrane association in serum-starved cells, suggestive evidence of elevated PtdIns(3,4)P_2 levels (data not shown). We have

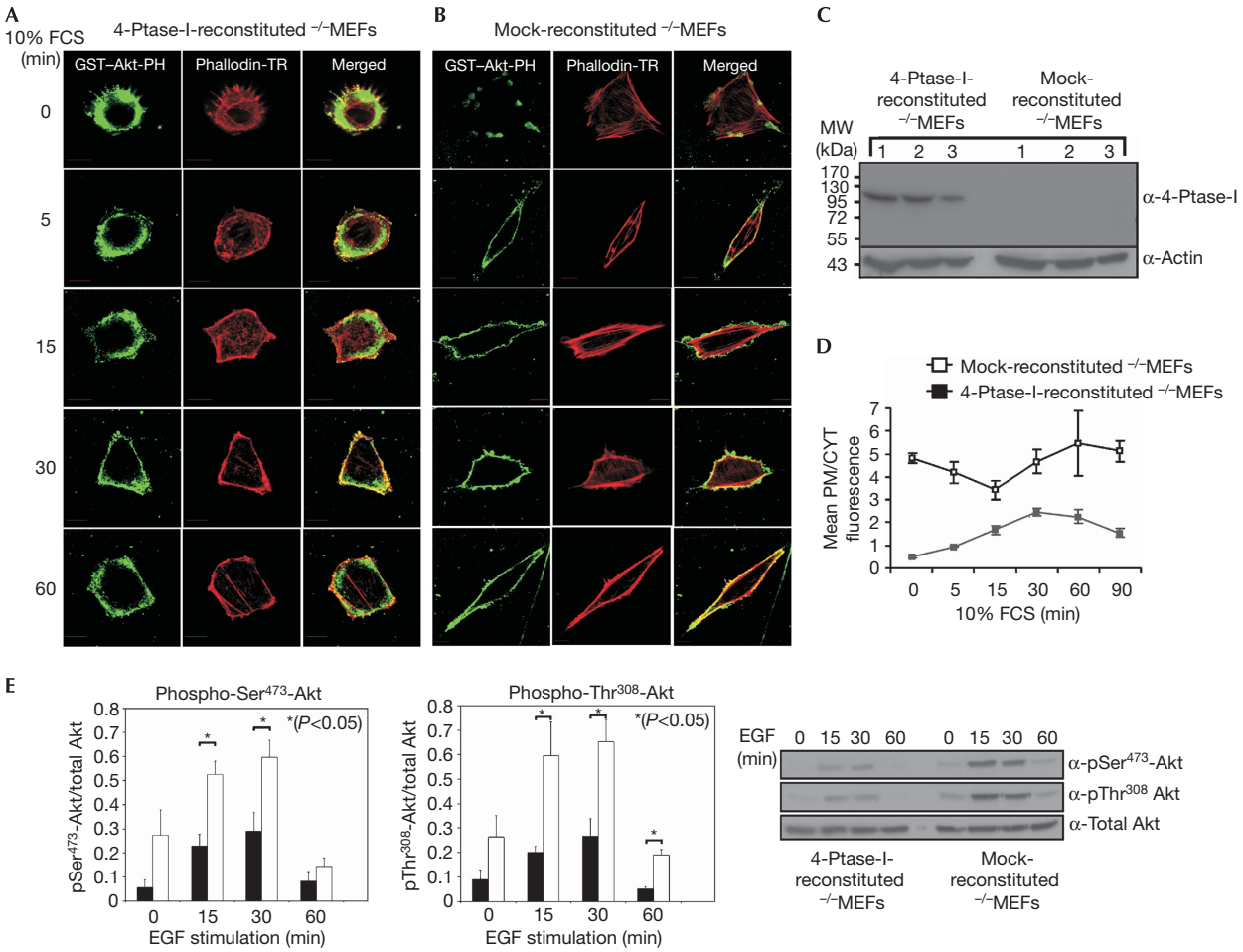

Fig 3 | Reconstitution of 4-ptase-1 rescues enhanced activation of Akt in $^{-/-}$MEFs. Immortalized $^{-/-}$MEFs reconstituted with (**A**) 4-ptase-1- or (**B**) mock-reconstituted $^{-/-}$MEFs were serum-starved overnight and stimulated with 10% FCS, fixed, digitonin-permeabilized and incubated with approximately 5 μg of GST-Akt/PH, followed by GST and rabbit Alexa-488 antibodies. Cells were imaged on an Olympus FV1000 confocal microscope under the same acquisition settings. Scale bar, 10 μm. (**C**) Whole-cell lysates from mock- or 4-ptase-1-reconstituted $^{-/-}$MEFs were immunoblotted in triplicate using 4-ptase-1 antibodies. (**D**) Mean intensity of GST-Akt/PH staining of four separate areas of approximately 150 pixels at the plasma membrane (PM) relative to the same size areas in the cytosol (CYT) of the same cell, for each time point (>20 cells), from four experiments was quantified using ImageJ software. (**E**) MEFs were serum-starved and 100 ng/ml of EGF treated and immunoblotted with pSer^{473}-Akt or pThr^{308}-Akt antibodies, analysed by densitometry and normalized to total Akt protein ($n=4$). EGF, epidermal growth factor; FCS, fetal calf serum; GST, glutathione *S*-transferase; MEF, mouse embryonic fibroblast; MW, molecular weight; PH, pleckstrin homology.

previously reported that the wild type, but not the catalytically inactive 4-ptase-1, can suppress the growth factor-stimulated generation of PtdIns(3,4)P_2, as assessed by the recruitment of GFP-PH-TAPP1 to the plasma membrane (Ivetac *et al*, 2005). In addition, in this previous study, we also measured the total cellular PtdIns(3,4)P_2 and PtdIns(3)P levels in cells overexpressing 4-ptase-1. Deacylated ^{32}P-labelled phosphoinositides were analysed by anion-exchange high-performance liquid chromatography. The expression of 4-ptase-1 reduced PtdIns(3,4)P_2 levels by 20% compared with the empty vector cells, with a 1.76-fold increase in PtdIns(3)P. A similar biochemical analysis of the lipid levels in *Weeble*, 4-ptase-1-deficient primary cells, has shown that PtdIns(3,4)P_2, but not PtdIns(3,4,5)P_3, signals were elevated relative to wild-type cells (Shin *et al*, 2005). Consistent with this, we reported here that the PtdIns(3,4,5)P_3 biosensors, Bruton's tyrosine kinase (Btk) and ARF nucleotide binding site opener (ARNO)-PH, showed similar membrane recruitment in $^{+/+}$MEFs and $^{-/-}$MEFs (data not shown). Therefore, it is likely that the enhanced activation of Akt observed in *Weeble* cells is a consequence of increases in PtdIns(3,4)P_2 signals owing to loss of its degradation by 4-ptase-1.

The 4-ptase-1-deficient *Weeble* mice show cerebellar dysfunction and ataxia, with increased apoptosis of neurons. Akt phosphorylation and signalling were not examined (Shin *et al*, 2005). The increased apoptosis in cerebellar postmitotic neurons, in contrast to the decreased apoptosis reported here in proliferating $^{-/-}$MEFs, might occur for reasons unrelated to the activity of Akt. RAB5, the small GTPase that forms a complex with 4-ptase-1, regulates clathrin-mediated endocytosis. *Weeble* neuron cell death might be due to decreased glutamate receptor endocytosis leading to increased excitatory signalling (Shin *et al*, 2005).

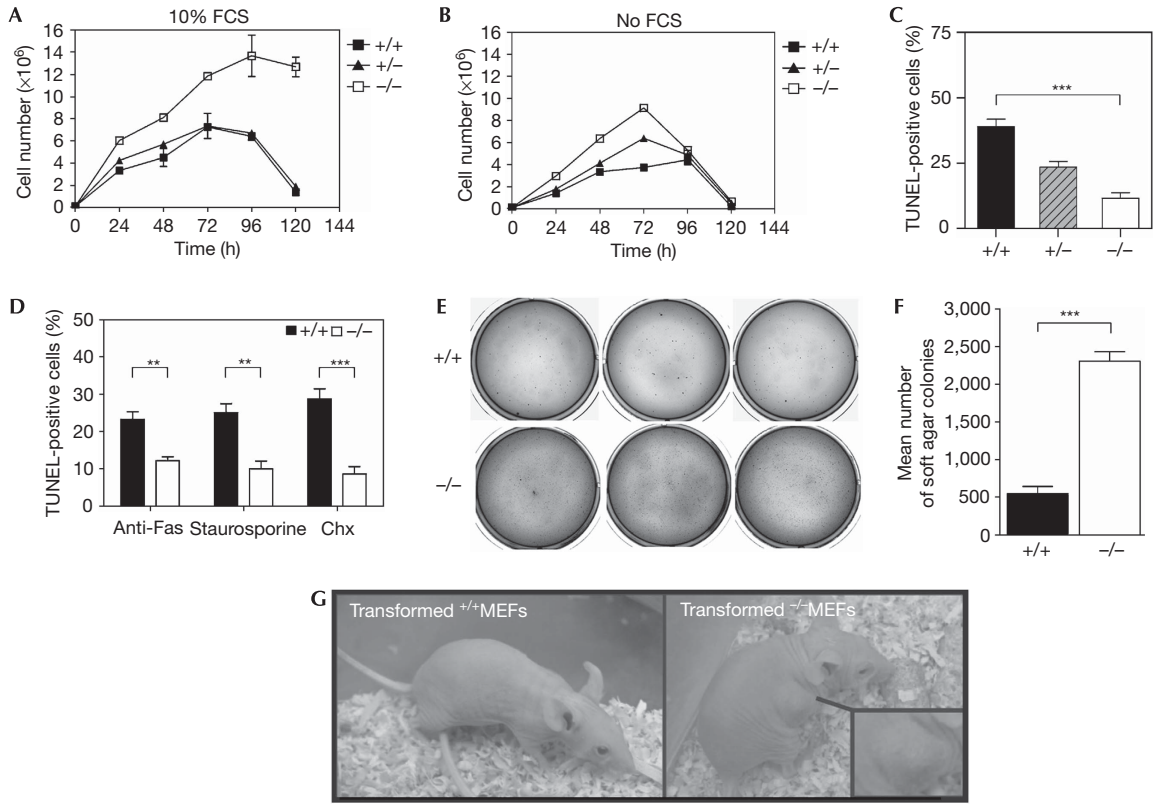

Fig 4 | $^{-/-}$MEFs show increased proliferation and decreased apoptosis. 1×10^5 log-phase growing primary MEFs were seeded in triplicate in the (**A**) presence or (**B**) absence of 10% FCS and counted daily ($n = 3$). (**C**) 3×10^5 primary MEFs were seeded in triplicate, serum-starved for 72 h and TUNEL-positive nuclei were scored as a proportion of total nuclei in six independent fields for three experiments (***$P < 0.001$). (**D**) 5×10^5 MEFs under normal growth conditions were treated with 1 μg/ml agonistic Fas antibodies, 1 μM staurosporine or 10 μg/ml cyclohexamide (Chx) for 8 h and analysed by TUNEL assay. Cells from six fields from three independent chambers were scored and normalized to no treatment control (***$P < 0.001$; **$P < 0.01$). (**E,F**) 1×10^4 SV40 large T antigen-transformed $^{+/+}$MEFs or $^{-/-}$MEFs were seeded in triplicate and grown in soft agar. Colonies with more than 50 cells were counted (***$P < 000.1$). (**G**) Mice were injected subcutaneously in the flank with SV40-transformed $^{+/+}$MEFs (no tumours in five mice), or $^{-/-}$MEFs (4/5 mice developed tumours, image of tumour magnified in box). FCS, fetal calf serum; MEF, mouse embryonic fibroblast; TUNEL, TdT-mediated dUTP nick end labelling.

Speculation

The PI(3)K/Akt pathway is frequently mutated and activated in tumours, and the PtdIns(3,4,5)P_3-3-ptase PTEN is a tumour suppressor (Tamguney & Stokoe, 2007). Gene profiling studies have identified altered 4-ptase-1 and -2 expression in human cancers, but the functional effects are uncharacterized (West *et al*, 2001; LaTulippe *et al*, 2002; Ross *et al*, 2003; Naylor *et al*, 2005; Barnache *et al*, 2006). An RNA-interference-based functional screen has identified 4-ptase-2 as a candidate tumour suppressor (Westbrook *et al*, 2005). A study using gene targeting by the Gr-1.4 virus to induce retroviral mutagenesis identified 4-ptase-1 as 1 of 79 candidate genes for acute myeloid leukaemia (Erkeland *et al*, 2004). It will be of great interest to analyse cancers for 4-ptase-1 or -2 mutations and/or altered expression and to evaluate for abnormal PI(3)K/Akt signalling. The 4-ptases, similar to PTEN, might represent tumour suppressor genes.

METHODS

DMEM, Optimem-I, Lipofectamine LTX, PLUS, phalloidin and Alexa-488 or -594-conjugated Ab were purchased from Invitrogen (San Diego, CA, USA). Rabbit and mouse HRP-conjugated antibodies were purchased from Silenus (Melbourne, Australia) and EGF from Millipore (Billerica, MA, USA). All other reagents were purchased from Sigma-Aldrich (St Louis, MO, USA).

Mammalian expression plasmids. The retroviral 4-ptase-1 construct was generated by subcloning of full-length 4-ptase-1 cDNA into the *Eco*RI site of p*Wzl*-Hygromycin vector. mCherry was from Roger Tsien (University of California, San Diego, USA).

Isolation of MEFs. MEFs were isolated from 13-day-old embryos (Ivetac *et al*, 2005). Low-passage (⩽P5) primary MEFs were used and genotyped as described previously (Nystuen *et al*, 2001).

Imaging. $^{+/+}$MEFs and $^{-/-}$MEFs were seeded at 2.5×10^4/ml onto round coverslips and co-transfected with GFP-Akt-PH and mCherry using Lipofectamine LTX. At 12–16 h post-transfection, cells were serum-starved for 2–4 h and imaged live using a Leica AF6000LX Live Cell Imaging Workstation, with a 63 × 1.3 water objective. Time-lapse fluorescence microscopy Monash Micro-imaging was performed at 1.5-min intervals under serum-starved conditions and following 10% FCS. Image analysis was performed using Metamorph software (Molecular Devices Corporation v7.1.3; adapted from Henry *et al*, 2004). Three regions of 100–500 pixels were outlined using the freehand tool at the site

of the plasma membrane GFP signal. A ratio image of GFP to mCherry average fluorescence of the same area at the plasma membrane ($R_{PM} = GFP_{PM} \times 1000/mCherry_{PM}$) was generated (divided image Fig 1D). Ratio images of 300 pixels of three areas in the cytosol ($R_{CYT} = GFP_{CYT} \times 1000/mCherry_{CYT}$) were generated. Normalized fluorescence was derived by calculating the R_{PM}/R_{CYT} ratio. Images were collected as 16-bit greyscale tagged image format (tif) files and prepared using ImageJv1.41 (http://rsbweb.nih.gov/ij/index.html).

MEFs grown on glass coverslips were fixed, permeabilized with 40 μg/ml digitonin for 20 min, washed and blocked in 3% BSA in PBS, incubated with GST-Akt-PH at 5 μg/μl for 30 min, washed and incubated with GST antibodies, followed by rabbit Alexa-488-conjugated antibodies.

Cell lysis and immunoblots. Cells were washed and lysed in 1% (v/v) Triton X-100 in 50 mM Tris, 150 mM NaCl, 1 mM benzamidine, 1 mM EDTA, 1 mM EGTA, 2.5 mM Na-pyrophosphate, 1 mM Na_3VO_4, 2 μg/ml leupeptin, 2 μg/ml aprotinin and 5 μg/ml pepstatin and Complete Mini Protease Cocktail Inhibitor Tablet (Roche, Penzberg, Germany). Lysates were extracted and pelleted. Protein (50 μg) was analysed by SDS–polyacrylamide gel electrophoresis (SDS–PAGE) and immunoblotted using ECL (Amersham, Amersham, UK). Western blot band intensities were analysed by densitometry and expressed as a fold increase relative to the wild-type genotype value at 0 min, arbitrarily defined as 1 and normalized to total Akt protein.

TUNEL apoptosis assay. MEFs seeded on eight-chamber slides were grown to subconfluence and serum-deprived or treated with 1 μg/ml agonistic Fas antibodies, 1 μM staurosporine or 10 μg/ml cycloheximide for 8–12 h. Apoptosis was detected by TUNEL using FLUORESCEIN *in situ* Cell Death Detection kit (Roche). Cells from six randomly chosen fields from three independent trials were scored for TUNEL-positive nuclei relative to total nuclei and normalized to no treatment control.

Anchorage-independent growth and tumorigenicity assays. Log-phase growing SV40 large T antigen-transformed MEFs were suspended in enriched medium (supplemented with 10% FCS and 1.5% agar) and plated onto the agar-coated six-well plates. Assays were performed in triplicate using two different starting cell concentrations of 2×10^3 and 1×10^4 cells/ml. After 4 weeks in culture, plates were stained with 0.01% crystal violet and colony numbers were scored. For tumorigenicity analysis, 100 μl PBS suspensions of 1×10^6 SV40-transformed $^{+/+}$MEFs or $^{-/-}$MEFs were injected subcutaneously into the flanks of ten 6-week-old athymic nude mice (*Balb/c*$^{nu/nu}$; five per genotype). The lengths and widths of tumours were determined using electronic calipers and the average tumour volumes were calculated using the formula (length × (breadth)^2/2).

CONFLICT OF INTEREST

The authors declare that they have no conflict of interest.

REFERENCES

Andjelkovic M, Alessi DR, Meier R, Fernandez A, Lamb NJ, Frech M, Cron P, Cohen P, Lucocq JM, Hemmings BA (1997) Role of translocation in the activation and function of protein kinase B. *J Biol Chem* **272:** 31515–31524

Astle MV, Seaton G, Davies EM, Fedele CG, Rahman P, Arsala L, Mitchell CA (2006) Regulation of phosphoinositide signaling by the inositol polyphosphate 5-phosphatases. *IUBMB Life* **58:** 451–456

Barnache S, Le Scolan E, Kosmider O, Denis N, Moreau-Gachelin F (2006) Phosphatidylinositol 4-phosphatase type II is an erythropoietin-responsive gene. *Oncogene* **25:** 1420–1423

Carpten JD *et al* (2007) A transforming mutation in the pleckstrin homology domain of AKT1 in cancer. *Nature* **448:** 439–444

Engelman JA, Luo J, Cantley LC (2006) The evolution of phosphatidylinositol 3-kinases as regulators of growth and metabolism. *Nat Rev Genet* **7:** 606–619

Erkeland SJ, Valkhof M, Heijmans-Antonissen C, van Hoven-Beijen A, Delwel R, Hermans MH, Touw IP (2004) Large-scale identification of disease genes involved in acute myeloid leukemia. *J Virol* **78:** 1971–1980

Franke TF, Kaplan DR, Cantley LC, Toker A (1997) Direct regulation of the Akt proto-oncogene product by phosphatidylinositol-3,4-bisphosphate. *Science* **275:** 665–668

Henry RM, Hoppe AD, Joshi N, Swanson JA (2004) The uniformity of phagosome maturation in macrophages. *J Cell Biol* **164:** 185–194

Ivetac I, Munday AD, Kisseleva MV, Zhang XM, Luff S, Tiganis T, Whisstock JC, Rowe T, Majerus PW, Mitchell CA (2005) The type Iα inositol polyphosphate 4-phosphatase generates and terminates phosphoinositide 3-kinase signals on endosomes and the plasma membrane. *Mol Biol Cell* **16:** 2218–2233

Kisseleva MV, Cao L, Majerus PW (2002) Phosphoinositide-specific inositol polyphosphate 5-phosphatase IV inhibits Akt/protein kinase B phosphorylation and leads to apoptotic cell death. *J Biol Chem* **277:** 6266–6272

LaTulippe E, Satagopan J, Smith A, Scher H, Scardino P, Reuter V, Gerald WL (2002) Comprehensive gene expression analysis of prostate cancer reveals distinct transcriptional programs associated with metastatic disease. *Cancer Res* **62:** 4499–4506

Manning BD, Cantley LC (2007) AKT/PKB signaling: navigating downstream. *Cell* **129:** 1261–1274

Naylor TL, Greshock J, Wang Y, Colligon T, Yu QC, Clemmer V, Zaks TZ, Weber BL (2005) High resolution genomic analysis of sporadic breast cancer using array-based comparative genomic hybridization. *Breast Cancer Res* **7:** R1186–R1198

Norris FA, Auethavekiat V, Majerus PW (1995) The isolation and characterization of cDNA encoding human and rat brain inositol polyphosphate 4-phosphatase. *J Biol Chem* **270:** 16128–16133

Norris FA, Atkins RC, Majerus PW (1997) The cDNA cloning and characterization of inositol polyphosphate 4-phosphatase type II. Evidence for conserved alternative splicing in the 4-phosphatase family. *J Biol Chem* **272:** 23859–23864

Nystuen A, Legare ME, Shultz LD, Frankel WN (2001) A null mutation in inositol polyphosphate 4-phosphatase type I causes selective neuronal loss in weeble mutant mice. *Neuron* **32:** 203–212

Ross ME *et al* (2003) Classification of pediatric acute lymphoblastic leukemia by gene expression profiling. *Blood* **102:** 2951–2959

Sarbassov DD, Guertin DA, Ali SM, Sabatini DM (2005) Phosphorylation and regulation of Akt/PKB by the rictor–mTOR complex. *Science* **307:** 1098–1101

Shin HW *et al* (2005) An enzymatic cascade of Rab5 effectors regulates phosphoinositide turnover in the endocytic pathway. *J Cell Biol* **170:** 607–618

Stephens L, Jackson T, Hawkins P (1993) Agonist-stimulated synthesis of phosphatidylinositol(3,4,5)-trisphosphate: a new intracellular signalling system? *Biochim Biophys Acta* **1179:** 27–75

Tamguney T, Stokoe D (2007) New insights into PTEN. *J Cell Sci* **120:** 4071–4079

Vyas P, Norris FA, Joseph R, Majerus PW, Orkin SH (2000) Inositol polyphosphate 4-phosphatase type I regulates cell growth downstream of transcription factor GATA-1. *Proc Natl Acad Sci USA* **97:** 13696–13701

West M, Blanchette C, Dressman H, Huang E, Ishida S, Spang R, Zuzan H, Olson JA Jr, Marks JR, Nevins JR (2001) Predicting the clinical status of human breast cancer by using gene expression profiles. *Proc Natl Acad Sci USA* **98:** 11462–11467

Westbrook TF *et al* (2005) A genetic screen for candidate tumour suppressors identifies REST. *Cell* **121:** 837–848